Redox Biology 38 (2021) 101784

Contents lists available at ScienceDirect

Redox Biology

journal homepage: www.elsevier.com/locate/redox

Research Paper

Vitamin E deficiency dysregulates thiols, amino acids and related molecules during zebrafish embryogenesis

Jie Zhang [a,b,1], Brian Head [a,c,1], Scott W. Leonard [a], Jaewoo Choi [a], Robyn L. Tanguay [d], Maret G. Traber [a,e,*]

[a] Linus Pauling Institute, Oregon State University, Corvallis, OR, USA
[b] College of Science, China Agriculture University, Beijing, China
[c] Molecular and Cell Biology Program, Oregon State University, Corvallis, OR, USA
[d] Department of Environmental Toxicology, College of Agricultural Sciences, Oregon State University, Corvallis, OR, USA
[e] School of Biological and Population Health Sciences, College of Public Health, Oregon State University, Corvallis, OR, USA

ARTICLE INFO

Keywords:
α-tocopherol
Choline
Betaine
Glutathione
Methyl donors

ABSTRACT

Vitamin E (α-tocopherol, VitE) was discovered as a nutrient essential to protect fetuses, but its molecular role in embryogenesis remains undefined. We hypothesize that the increased lipid peroxidation due to VitE deficiency drives a complex mechanism of overlapping biochemical pathways needed to maintain glutathione (GSH) homeostasis that is dependent on betaine and its methyl group donation. We assess amino acids and thiol changes that occur during embryogenesis [12, 24 and 48 h post fertilization (hpf)] in VitE-sufficient (E+) and deficient (E−) embryos using two separate, novel protocols to quantitate changes using UPLC-MS/MS. Using partial least squares discriminant analysis, we found that betaine is a critical feature separating embryos by VitE status and is higher in E− embryos at all time points. Other important features include: glutamic acid, increased in E− embryos at 12 hpf; choline, decreased in E− embryos at 24 hpf; GSH, decreased in E− embryos at 48 hpf. By 48 hpf, GSH was significantly lower in E− embryos ($P < 0.01$), as were both S-adenosylmethionine (SAM, $P < 0.05$) and S-adenosylhomocysteine (SAH, $P < 0.05$), while glutamic acid was increased ($P < 0.01$). Since GSH synthesis requires cysteine (which was unchanged), these data suggest that both the conversion of homocysteine and the uptake of cystine via the X_c^- exchanger are dysregulated. Our data clearly demonstrates the highly inter-related dependence of methyl donors (choline, betaine, SAM) and the methionine cycle for maintenance of thiol homeostasis. Additional quantitative flux studies are needed to clarify the quantitative importance of these routes.

1. Introduction

Vitamin E (α-tocopherol, VitE) was discovered because it is a necessary nutrient to maintain pregnancy in rats [1]. Importantly, VitE sufficiency is closely associated with the developing nervous system in poultry [2], rodents [3], and zebrafish [4]. In particular, zebrafish embryos are a frequently used model for developmental biology given they develop externally, are transparent, easy to maintain and are produced in large quantities to allow sensitive analyses [5]. The fertilized egg contains all of the necessary nutrients and is a self-contained unit that develops into a swimming fish in 5 days. Therefore, we developed a unique model of VitE deficiency using zebrafish embryos obtained by spawning adult fish fed VitE deficient (E−) diets.

The use of E− embryos has allowed study of the interactions of interdependent, overlapping metabolic systems during embryonic development [6–9]. Critically, by 5 days 80% of E− embryos have morphologic abnormalities or have died [8]. Not surprisingly, since VitE is a lipid soluble, peroxyl radical scavenger, E− embryos experience lipid peroxidation, depletion of phosphatidyl choline with docosahexaenoic acid (DHA-PC) and dysregulated phospholipid metabolism [8,10]. Additionally, we reported using targeted metabolomics analyses over a time course of 5 days that E− embryos had dysregulated energy metabolism [8], as well as mitochondrial dysfunction, measured by extracellular oxygen consumption [8]. Specifically, glucose was depleted and its supplementation could partially rescue the E− embryos [8,9]. We also found in E− embryos that choline was depleted by 24 h

* Corresponding author. Linus Pauling Institute, 307 LPSC Oregon State University Corvallis, OR, 97330, USA.
E-mail address: maret.traber@oregonstate.edu (M.G. Traber).
[1] Brian Head and Jie Zhang contributed equally to this work.

https://doi.org/10.1016/j.redox.2020.101784
Received 27 October 2020; Accepted 1 November 2020
Available online 4 November 2020

post-fertilization (hpf) and that over time betaine became dysregulated, along with glutathione (GSH) depletion [8,9]. Moazzami et al. [11], who utilized non-targeted ^{1}H-NMR-metabolomics to investigate long-term effects of VitE deficiency in rats, also found that betaine concentrations were higher and expression of genes related to energy metabolism were lower in deficient rats. Taken together, these data show that VitE is necessary to maintain energy homeostasis, and also point to betaine as a critical nutrient that becomes dysregulated as deficiency proceeds.

Dysregulation of betaine concentrations in E− embryos is consequential because betaine is a methyl donor that plays a significant role in zebrafish development. Betaine homocysteine S-methyltransferase (BHMT, EC 2.1.1.5) catalyzes the transfer of methyl groups from betaine to homocysteine (Hcy) to form methionine (Met). Yang et al. [12] showed that the *bhmt* gene is highly expressed at 12, 24 and 72 hpf in zebrafish embryos. Additionally, cystathionine β-synthase (CBS, EC 4.2.1.22) catalyzes the first step of the transsulfuration pathway, converting Hcy to cystathionine. *Cbs* knockdown in zebrafish causes a bent embryonic axis that can be rescued with betaine [13]. Thus, understanding betaine regulation may provide a critical linkage between metabolic pathways and thiol redox status to define the consequences of VitE deficiency.

This linkage between VitE deficiency, increased lipid peroxidation and thiol status has been studied in E− embryos using lipidomics [10] and metabolomics [8]. These latter studies suggested that choline, betaine and the methionine cycle were dysregulated by inadequate VitE protection during embryogenesis. The dysregulation of these pathways in E− embryos causes abnormal nervous system formation, especially the midbrain-hindbrain boundary, spinal cord and dorsal root ganglia [14]. Thus, we raise the question "why is a water-soluble methyl donor dysregulated during VitE deficiency?" We hypothesize that an increased requirement for GSH during the increased lipid peroxidation observed in E− embryos drives a complex mechanism of overlapping biochemical pathways needed to maintain thiol homeostasis that is dependent on betaine and methyl group donation. To test this hypothesis, we have developed highly sensitive, analytical methodologies to measure both critical amino acids and thiols, longitudinally in E− and E+ zebrafish embryos.

2. Materials and METHODS

2.1. Materials and reagents

Supplies were obtained as follows: ammonium formate (Optima, Fisher); formic acid (Optima LC-MS grade, Fisher Chemical); tris (2-carboxyethyl) phosphine hydrochloride (TCEP, Sigma-Aldrich); N-ethylmaleimide (NEM; Sigma-Aldrich); ethylenediaminetetraacetic acid (EDTA; EMD Millipore); 5-sulfosalicylic acid (SSA; Sigma-Aldrich); zirconium oxide beads (Next Advance); amino acid standard mix (Sigma-Aldrich); stable isotope-labeled amino acid standard mix (Cambridge Isotope); choline chloride (Fluka); betaine (Sigma-Aldrich); S-adenosylmethionine (SAM) (Cayman Chemical); S-adenosylhomocysteine (SAH) (Cayman Chemical). The stable isotope-labeled internal standard (IS) GSH-(glycine-$^{13}C_2$, ^{15}N) trifluoroacetate salt (Sigma-Aldrich, St Louis, MO) was used for recovery analysis and quantitation of free thiols. All other reagents and solvents were of analytical grade.

2.2. Zebrafish husbandry

The Institutional Animal Care and Use Committee (IACUC) of Oregon State University approved the protocol (ACUP Number #5068). Tropical 5D strain zebrafish were reared in the Sinnhuber Aquatic Research Laboratory at Oregon State University under standard laboratory conditions of 28 °C on a 14-h light/10-h dark photoperiod according to standard zebrafish breeding protocols [15]. At 55 days post-fertilization, adult zebrafish were randomly allocated to one of two experimental diets, VitE deficient (E−) or sufficient (500 mg RRR-α-tocopheryl acetate/kg diet, E+), as previously described [7,8,16]. We obtained E− and E+ embryos by spawning adult 5D zebrafish that had been fed either E− or E+ diets, respectively, for a minimum of 80 days. Control embryos were obtained from adults fed standard zebrafish food (Gemma micro, https://zebrafish.skrettingusa.com/). Diet and embryo α- and γ-tocopherol concentrations (Supplement Table 1) were determined using high-performance liquid chromatography with electrochemical detection [17].

Embryos were collected, staged and incubated in standard embryo media (EM; reverse osmosis water with 15 mM NaCl, 0.5 mM KCl, 1 mM $CaCl_2$, 1 mM $MgSO_4$, 0.15 mM KH_2PO_4, 0.05 mM Na_2HPO_4 and 0.7 mM $NaHCO_3$) [18]. Reproductive output was determined by pair spawning females followed by total egg count per female. For extraction protocols, only living embryos as evaluated by spontaneous embryo movement were used for analysis and these embryos were randomly sampled from those viable at the given sampling time. To reduce variability due to differences in hatching, all embryos used for analysis were unhatched with chorion on to investigate changes unrelated to hatching, which may significantly alter the embryos' redox potential [19]. For sample preparation, embryos at 12, 24 and 48 hpf were transferred to 1.7 ml microcentrifuge tubes. The tubes were kept on ice for 30 min to euthanize the animals, the liquid removed, and prepared as described below, then the samples were snap frozen in liquid nitrogen and stored at −80 °C. Live embryos were used for morphological assessment. At 12, 24 and 48 hpf, embryos were mounted in 3% methylcellulose on a glass slide dish, anesthetized with tricaine and imaged using a Keyence BZ-x700 All-in-One Microscope. Images were taken with the 2× and 10× objective using brightfield imaging. All image enhancements (contrast, saturation) were made uniformly in Adobe Photoshop. Egg traits were assessed by egg yolk diameter followed by egg volume estimated based on the volume of an ellipsoid using the equation [20,21]:

$$Volume = \frac{4}{3}\pi \times (small\ axis\ radius) \times (large\ axis\ radius)^2$$

2.3. Thiol extraction and determination by UPLC-MS/MS

Free thiols in embryos were extracted, derivatized and measured by UPLC-MS/MS, as adapted from Ref. [6–8]. The extracted and quantitated thiols included GSH, glutathione disulfide (GSSG), cysteine, homocysteine (Hcy), and cystine (cysteine disulfide, CysS). Briefly, embryos (n = 10) were homogenized in the derivatizing and protein precipitating solution (20 mM NEM, 50 mM EDTA and 2% SSA in 15% methanol, final concentrations) using a bullet blender (Next Advance, Inc. Troy, NY) with 0.5 mm zirconium oxide beads for 2 min at speed 10. Prior to homogenization, an aliquot of the internal standard (IS) [GSH–(glycine-$^{13}C_2$, ^{15}N)] was added to each sample for quantitation and to correct for non-specific losses.

NEM incubation times between 1 min and 1 h have been previously reported for a variety of biological samples, including red blood cells and human plasma [22], but we found that this length of time was insufficient for the more complex whole zebrafish embryo homogenate. To determine the optimal length of time necessary for complete thiol derivatization with NEM, a time course was performed. The minimum time necessary for maximum derivatization was 9 h (see below). The reaction can continue at room temperature protected from light for up to 24 h after homogenization with thederivatizing solution without any subsequent increase in oxidation of GSH to GSSG (see below). For the data in this report, the embryo homogenate and derivatizing solution mixture were incubated at room temperature for a minimum of 9 h. Following derivatization, samples were centrifuged at room temperature for 5 min at 14,000 rpm. Supernatants were transferred to injection vials, then stored at 10 °C until UPLC-MS/MS analysis.

Derivatized-thiols and thiol disulfides were separated using a C18 column [temperature 40 °C, Acquity UPLC BEH© C18 (2.1 × 100 mm × 1.7 μm; Waters, Milford, MA)] and a UPLC (Waters Acquity H system)

coupled with a Xevo TQD mass spectrometer (Waters, Milford, MA) equipped with an electrospray ionization source operated in positive mode (ESI+). MS tune conditions were as follows: desolvation gas 800 L/h; capillary 2.00 kV; cone 37 V; ESI + probe temperature 500 °C. MassLynx v.4.1 software (Waters, Milford, MA) was used for instrument control and data acquisition. Analytes were detected and quantified by multiple reaction monitoring (MRM). Chromatographic separation was achieved at a flow-rate of 0.375 mL/min using a gradient with mobile phase A (MP A, water with 0.1% formic acid) and mobile phase B (MP B, acetonitrile with 0.1% formic acid), as follows: Initial conditions were 0% MP B increased by slight convex curve to 60% for 1.10 min. After 1.10 min a gradient was initiated for 0.2 min (1.10–1.30 min), and MP B was increased linearly to 95%. From 1.30 to 1.67 min MP B was held at 95%. At 2.14 min MP B was increased to 100% and held at 100% until 4.0 min, then solvents were returned to initial conditions. Total run time was 5 min including column equilibration. The MRM-transitions and retention times of the individual derivatized thiols and thiol disulfides are shown in Supplement Table 2. Standard curves were linear ($r^2 \geq 0.98$) between 10 fmol and 100 pmol injected for all thiols tested.

To determine extraction efficiency, derivatization and recovery of NEM-conjugated free thiols, zebrafish embryo pools (n = 5 pools, 10 embryos per pool) were spiked with known IS concentrations at two points in the high (50–100 pmol injected) and two points in the low (0.5–1 pmol injected) end of the standard curve. The embryo pools were then homogenized in derivatizing solution and measured, as described. Recovery was calculated:

$$Recovery = 100 \times [(sample\ analyte + IS) - sample\ analyte] \,/\, IS$$

2.4. Assessment of thiol extraction and quantitation method development

Embryo pools were homogenized in derivatizing solution, then at periodic intervals (1, 2, 3, 6, 9, 12 and 24 h) samples were centrifuged, supernatants were transferred to injection vials and subjected to analysis. Labeled internal standard (IS) added to the standard curve was used to estimate maximum derivatization in the absence of the embryo homogenate, which presumably was caused by matrix effects in those homogenates. We determined that the half-life to the maximum derivatization of homogenates was 3.3 h and was similar for all thiols tested. By 9 h nearly 90% of free thiols in the sample were derivatized with NEM. Using the 9 h incubation protocol, the recovery of added standard to sample homogenates were consistently >75% for all analyses at two points in the high [50–100 pmol injected] and two points in the low [0.5–1 pmol injected] end of the standard curve. Thus, a solution containing SSA, EDTA and NEM effectively protects 90% of free thiols in zebrafish embryo homogenates without any increase in GSSG.

2.5. Analysis of amino acid and related metabolites

To extract amino acids and related compounds from embryos, 50 μL TCEP (100 mg/ml) and 350 μl acetonitrile were added to 1.7 ml microcentrifuge tubes each containing 10 embryos. The samples were homogenized with 0.5 mm zirconium oxide beads using a bullet blender for 3 min, at speed 10, then centrifuged at 4 °C at 15,000 × *g* for 5 min. An appropriate aliquot of the supernatant was diluted with Mobile Phase B (MP B, 10 mM ammonium formate in 85% acetonitrile) and IS containing multiple-labeled amino acids added. An aliquot was transferred to low volume injection vials and stored at −80 °C until LC-MS/MS analysis.

Amino acids and related compounds were analyzed, as described [23] with modifications, using the UPLC-MS/MS equipment described above. The MS/MS was operated in ESI + mode with equipment parameter settings as follows: desolvation gas 1000 L/h, capillary voltage 1.00 kV, desolvation temperature 550 °C and cone gas flow 10 L/h. Collision energy (CE) and cone voltage were optimized for each compound of interest and analyzed using MRM. The column used was a BEH Amide (Waters® Acquity UPLC 1.7 μM, 2.1 × 100 mm) with a VanGuard guard column (Waters® Acquity UPLC 1.7 μM, 2.1 × 5 mm). The column was maintained at a temperature of 40 °C. Optimal chromatographic separation was achieved at a flowrate of 0.3 mL/min using a gradient with mobile phase C (MP C, 10 mM ammonium formate) and MP D as follows: initial conditions were 100% MP D, hold 6 min. After 6 min a gradient was initiated for 0.1 min (6.0–6.1 min), then MP D was decreased to 94.1%. From 6.1 to 10 min MP D was linearly decreased to 82.4% and from 10 to 14 min, MP D was decreased to 70.6%. After 14 min solvents were returned to the initial conditions. Total run time was 20 min including column equilibration. MassLynx v.4.1 software was used for instrument control and data acquisition. Retention times, MRM transitions and CE are shown for the unlabeled and labeled analytes (Supplement Table 3). The range of linearity (pmol/injected) and correlation coefficients for the standard curves are shown in Supplement Table 4.

2.6. Repeatability and reproducibility of measurements: thiols, amino acids and related metabolites

Measurements of triplicates varied <10%; this variation is within acceptable limits set by the ICH calling for 3 replicates each at 3 test concentrations with variation of ±20% [24]. Inter-day assessments were made with thiols extracted and derivatized from three zebrafish homogenate pool of 24 hpf embryos analyzed five times. Derivatized analytes (GSH, cysteine and homocysteine) had between day % coefficient of variation (CV) in the range of 2.3–7.2% (Supplement Table 5). Within-day precision was also calculated with one zebrafish homogenate pool of 24 hpf embryos analyzed 5-times resulting in %CV values ranging from 2.7 to 11.7%. The %CV for amino acid (AA) quantitation of five replicate injections of standards on one day ranged from 1.1 to 12.3%. The %CV ranged from 0.8 to 16.1% when the standards were injected on three different days. Higher %CV were observed for those compounds [S-adenosylhomocysteine (SAH), S-adenosylmethionine (SAM), choline and betaine] for which no labeled IS was available. The highest within day %CV of this latter group (20.8%) was observed for SAH, which is present at low concentrations in embryos (Supplement Table 6).

2.7. Statistical analyses, principal component analyses and hierarchical clustering

We validated our outcomes by assessing 1) sensitivity [limits of detection (LOD) and of quantification (LOQ)], 2) accuracy and precision, and 3) recovery of authentic standards added to embryos prior to extraction. LOD and LOQ were established with signal-to-noise ratio (S/N) of 3/1 and 10/1, respectively (consistent with the International Council for Harmonization of Technical Requirements for Pharmaceuticals for Human Use (ICH) standards [24]). Precision (CV%) of inter- and intra-day assays was measured and calculated by replicate analysis (n = 5 or 3, as indicated). For thiol analyses, labeled GSH-($^{13}C_2$–^{15}N) was used as an IS to determine derivatization efficiency and recovery throughout method development and sample analysis. For amino acid analysis, labeled IS additions for most analytes were used. Results for both assays were corrected for IS recovery with quantitation relative to the respective standard curves.

Data from both analyses were combined into one dataset. All data (metabolite concentrations per embryo) were normalized by log transformation and auto scaling prior to statistical analysis. Two-dimensional (2D) principal component analysis (PCA) score and loading plots were generated by MetaboAnalyst 3.0 (https://www.metaboanalyst.ca/) [25,26]. Comparisons were made at each independent time point between diet groups using a supervised partial least squares-discriminant analysis (PLSDA) clustering method. PLSDA variable of importance (VIP) features were generated to identify metabolites that differentiate the diet groups. Heatmaps were generated between E+ and E− diet groups.

Hierarchical clustering was performed using the Ward algorithm and separated by Euclidean distance with factors visually arranged by time point. Statistical differences between groups, over time were assessed using 2-way ANOVA with Tukey's multiple comparison tests (Prism 6.0, GraphPad, La Jolla, CA). Statistical significance between differences was set at $P < 0.05$. Differences between reproductive output and egg yolk volume in 3 hpf embryos was assessed with t-tests between E+ and E− groups. Data are reported as group mean ± standard error of the mean (SEM).

3. Results

3.1. Embryo morphology and egg quality assessment

E+ and E− embryos were first assessed for proper development by morphologic screening at 12, 24 and 48 hpf with representative embryos shown (Fig. 1). E+ embryos at 12 hpf were developmentally normal with 5–6 somites located dorsally in addition to anterior head and eye (Fig. 1A). E− embryos, however, were noticeably delayed, as shown by reduced somite progression (Fig. 1B, *). By 24 hpf, E+ embryos had tightly packed V-shaped myotomes distributed throughout the trunk, defined eyes and early otic vesicle, and extended tails (Fig. 1C). E− embryos (24 hpf) had loosely packed myotomes and reduced tail extension (Fig. 1D, *). At 48 hpf, E+ embryos are developmentally normal, indicated by pigment cell migration dorso-laterally, circulation present in the pericardium and a straight notochord extending from head to tail (Fig. 1E). E− embryos (48 hpf) experience greater incidence of both yolk sac and pericardial edema (*) and bent axis (Fig. 1F). To determine if initial maternal contribution and initial egg quality predicts embryonic morphological deformities, reproductive parameters were assessed. E+ and E− females at approximately 1 year old, and 9 months on diet produced similar numbers of eggs with 67.4 ± 7.7 eggs per E+ female and 75.7 ± 17.8 eggs per E− female (mean ± SEM, $p = 0.674$, n = 7 and 13, respectively). Egg quality was assessed at 3 hpf (1 thousand-cell stage) prior to onset of any visible morphological abnormalities in either group. Egg yolk volume was found to be similar between embryos (E+, 0.155 ± 0.003 mm^3 vs E−, 0.153 ± 0.006 mm^3; $p = 0.758$, n = 7 per group).

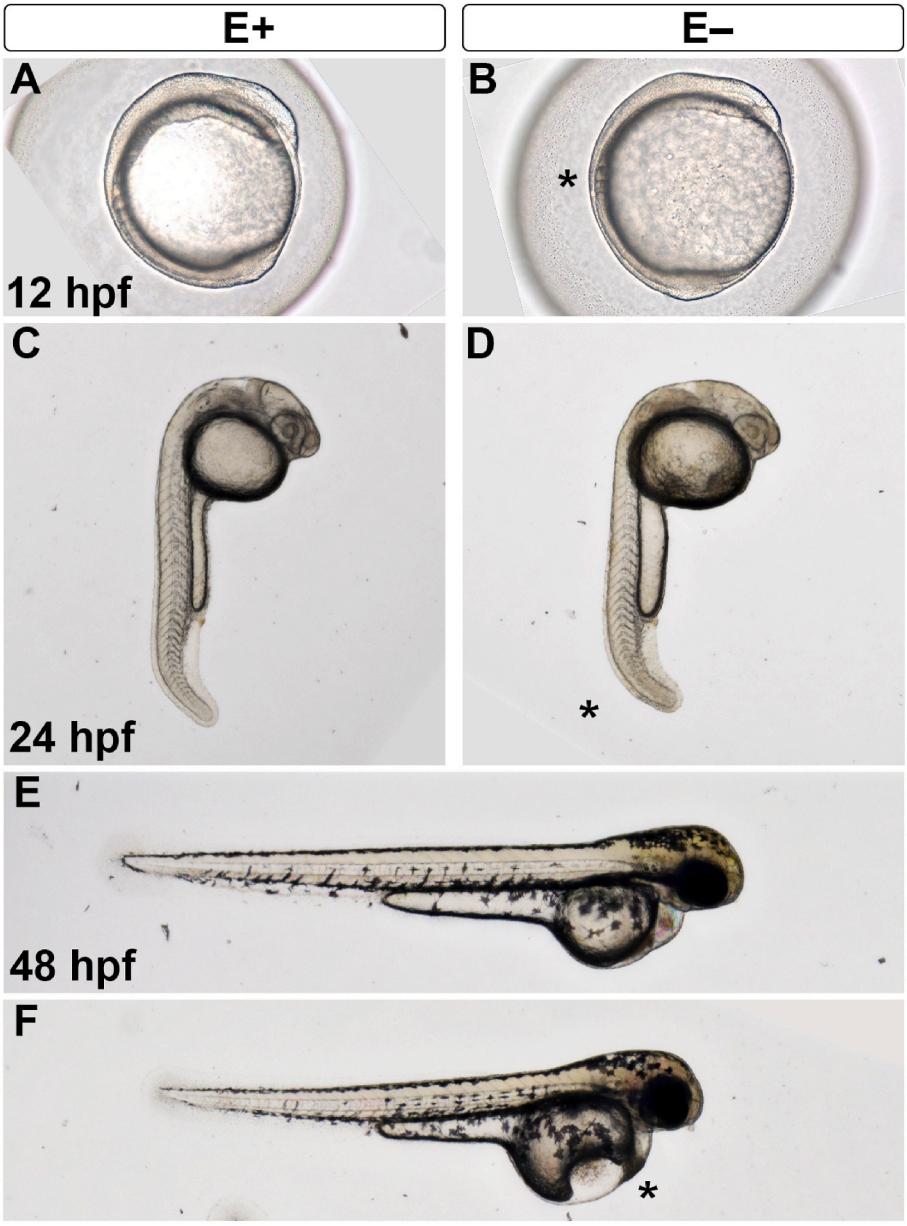

Fig. 1. Embryos are similar sized at each stage with E− developmentally delayed.
Live imaging of embryos was performed at each developmental stage used for assays and shows that embryos are of similar size, as measured by egg diameter, egg yolk diameter and estimated egg yolk volume. At 12 hpf, E+ embryos (A) develop normally indicated by 5–6 somites. At the same stage, E− embryos (B) are developmentally delayed with reduced somites (*) and smaller anterior head region. By 24 hpf, the otic vesicle is apparent, myotomes are neatly packed in V-shapes and the tail begins to extend in E+ embryos (C). In a representative E− embryo, however, the otic vesicle is less visible, posterior myotomes are loosely packed and the tail extension is reduced (D, *). E+ embryos at 48 hpf (E) show pigment migration dorso-laterally and have experienced the first heartbeat with visible circulation in the pericardium. E− embryos at the same stage (F) have greater incidence of both yolk sac and pericardial edema (*). (A-B) are taken with a 10× objective, (C–F) are taken with a 2× objective. Image was generated in Adobe Photoshop and any manipulations (contrast, saturation) were performed uniformly across images at the same developmental stage.

3.2. Impact of VitE deficiency on GSH and GSSG

Embryo GSH concentrations increased in all groups from 12 to 24 hpf. In control and E+ embryos, GSH concentrations remained elevated between 24 and 48 hpf (Table 1). By contrast, at 48 hpf GSH concentrations decreased in the E− embryos. The GSH/GSSG ratio, which provides a measure of redox status, is very high (2500–4500 mol/mol) up to 24 hpf in all groups. By 48 hpf, the ratios decreased in all groups to <725 mol/mol.

3.3. Integrated analysis of thiols and amino acids

To evaluate how VitE deficiency and the changes in thiol redox status altered free amino acid composition, quantitative assays were used to measure longitudinal (12, 24, 48 hpf) changes in E+ and E− zebrafish embryos. The thiol and the amino acid data from the same embryo cohorts were combined and evaluated using PLSDA. This analysis maximizes covariance between the metabolite features and VitE status, such that sample clusters are expected to separate with 95% confidence regions (CR) at each time point (12, 24 and 48 hpf). Component 1 describes metabolite features and component 2 describes treatment groups. At 12 hpf, component 1 accounts for 54.2% of the variation and component 2 accounts for 16.6% of the variation (Fig. 2A). The Q^2 index was greater than 0.90 with 4 components indicating excellent model fit. Top VIP scores indicating most important features that were high in abundance in E− embryos at 12 hpf were betaine, glutamic acid, serine and histidine; by contrast, SAM was low in E− embryos (Fig. 2B). At 24 hpf, E+ and E− embryos again clustered separately with non-overlapping CR (Fig. 2C). Components 1 and 2 account for 43.1% and 24.3% of the variation, respectively. The Q^2 index was greater than 0.90 with 4 components. Betaine, which was higher in E− embryos at 24 hpf, remained the most important feature separating embryo groups. Importantly, choline, threonine and tyrosine were all greater in E+ relative to E− embryos (Fig. 2D). At 48 hpf, components 1 and 2 account for 15.7% and 57.7% of the variation, respectively (Fig. 2E). The Q^2 index was greatest with 3 components indicating excellent fit. Top VIP scores metabolites in E+ embryos include GSH and SAH with higher abundant metabolites in E− embryos including betaine and glutamic acid.

Table 1
GSH and GSSG concentrations (pmol/embryo) over time by embryo group.

Embryo group	GSH[1]	GSSG[2]	GSH:GSSG[3]
Control			
12 hpf	569 ± 18	0.13 ± 0.01[a]	4547 ± 432[a]
24 hpf	747 ± 37[a]	0.30 ± 0.05[a]	2678 ± 388 [b]
48 hpf	809 ± 37[a]	1.14 ± 0.07	717 ± 52[c]
E + l			
12 hpf	454 ± 13	0.13 ± 0.01[a]	3514 ± 317[a]
24 hpf	709 ± 27[a]	0.18 ± 0.01[a]	4113 ± 325[a,b]
48 hpf	656 ± 30[a]	0.99 ± 0.09	690 ± 82[c]
E–l			
12 hpf	489 ± 9[a]	0.12 ± 0.00[a]	4185 ± 244[a]
24 hpf	695 ± 11[b]	0.28 ± 0.04[a]	2771 ± 475 [b]
48 hpf	529 ± 21[a]	1.11 ± 0.11	489 ± 41[c]

Concentrations are shown for GSH and GSSG (pmol/embryo, mean ± SEM, n=5 group per time).
[1]GSH: Interaction, $P<0.0001$; For the E+ vs E– comparisons: at 12 and 24 hpf, NS; 48 hpf, $P<0.01$. Within each group, values that do not share the same letter are different ($P<0.001$) at the indicated times.
[2]GSSG, time main effect $P<0.0001$. Within each group, values that do not share the same letter are different ($P<0.001$) at the indicated times
[3]GSH:GSSG (mol:mol ± SEM, n=5 per time point): interaction $P=0.0045$; values were significantly different ($P<0.05$) 12 vs 24, except NS for the E+ 12 and 24 hpf comparison; all other times within each group, $P<0.001$.

3.4. Hierarchical clustering of E+ and E− outcomes

Hierarchical clustering was used to classify the metabolite features into related groups (Fig. 3). A dendrogram was used to sort the metabolites (rows) according to similarities in their patterns using the Ward clustering algorithm, while the color scheme from blue (lowest) to peach (highest) show the relative concentrations. Each of the time intervals (12, 24, and 48 hpf) is indicated for the E+ and E− embryos. In general, the compounds increased with embryo developmental age except for choline, cysteine, SAH, SAM, which were lower at 48 than at 24 hpf. These latter compounds clustered at the top of the heatmap. Glutamate and homocysteine (Hcy) clustered together and with the previous grouping. Betaine and GSSG clustered together and increased with time as shown by the dark peach color at 48 hpf. (Fig. 3). Cystine showed a similar pattern, but was located further down in the heat map. Of note, compounds (GSH, serine, proline and isoleucine) clustered together near the middle of the heat map showed similar trends. The compounds that clustered in the bottom of the figure were methionine, leucine, phenylalanine, threonine, tyrosine, valine, lysine, arginine, alanine, and histidine, which were correlated with each other.

3.5. Pathways relating AA and thiol status of E+ and E− embryos

Betaine and GSSG are oxidation products of choline and GSH, respectively; therefore, we have integrated our data with the metabolic pathways leading from choline and betaine to GSH and GSSG. The concentrations of the thiols and AA were measured in a single batch of control, E+ and E− embryos at 12, 24 and 48 hpf (Fig. 4). We particularly focused on the two pathways to maintain cysteine concentrations because cysteine is the rate limiting amino acid for GSH synthesis. Notably, cysteine concentrations were unchanged between E+ and E− embryos, while by 48 hpf GSH concentrations were significantly ($P <$ 0.01) lower in E− (529 ± 21 pmol/embryo) compared with E+ embryos (655 ± 30 pmol/embryo, Table 1, Fig. 4). AA levels varied by time, with most reaching their highest concentrations at 24 hpf. Choline showed no apparent differences among control, E+ and E− embryos. By contrast, betaine in E− embryos significantly increased at each of the time points: 12, 24 and 48 hpf, and were 6.7-, 2.0- and 1.6-fold higher than in E+ embryos, respectively. By contrast, SAM and SAH significantly decreased at 48 hpf in E− compared to E+ embryos, with 0.58- and 0.57-fold changes, respectively. Although methionine increased significantly with time, no statistical differences were found between the groups. Early (12 hpf) significant changes in E− embryos were observed for serine (1.3-fold increase compared to E+) and glutamate (1.4-fold increase compared to E+). Additionally, glutamate concentrations were higher in 48 hpf E− embryos (1.4-fold compared to E+). Although threonine, alanine, tyrosine, isoleucine, leucine, phenylalanine, lysine, arginine and histidine significantly increased with time, no differences were found in the concentrations in control, E+ and E− embryos (Fig. S1). E+ embryos at 12 hpf showed significantly higher proline than in control samples (1.30-fold increase). At 24 hpf, valine in E− embryos decreased significantly compared to the control (0.81-fold change) (Fig. S1).

4. Discussion

We hypothesized that the requirement for GSH during the increased lipid peroxidation observed in E− embryos drives a complex mechanism of overlapping biochemical pathways needed to maintain thiol homeostasis that is dependent on betaine and methyl group donation. Using sensitive extraction and quantitation techniques has allowed us to evaluate the global changes in thiol and amino acids in response to VitE deficiency over time. Previously, we showed that thiol status was dysregulated in E− embryos [8,9]. The present studies extend those observations to quantitative thiol measurements along with accurate quantitation of embryo AA at critical developmental time points.

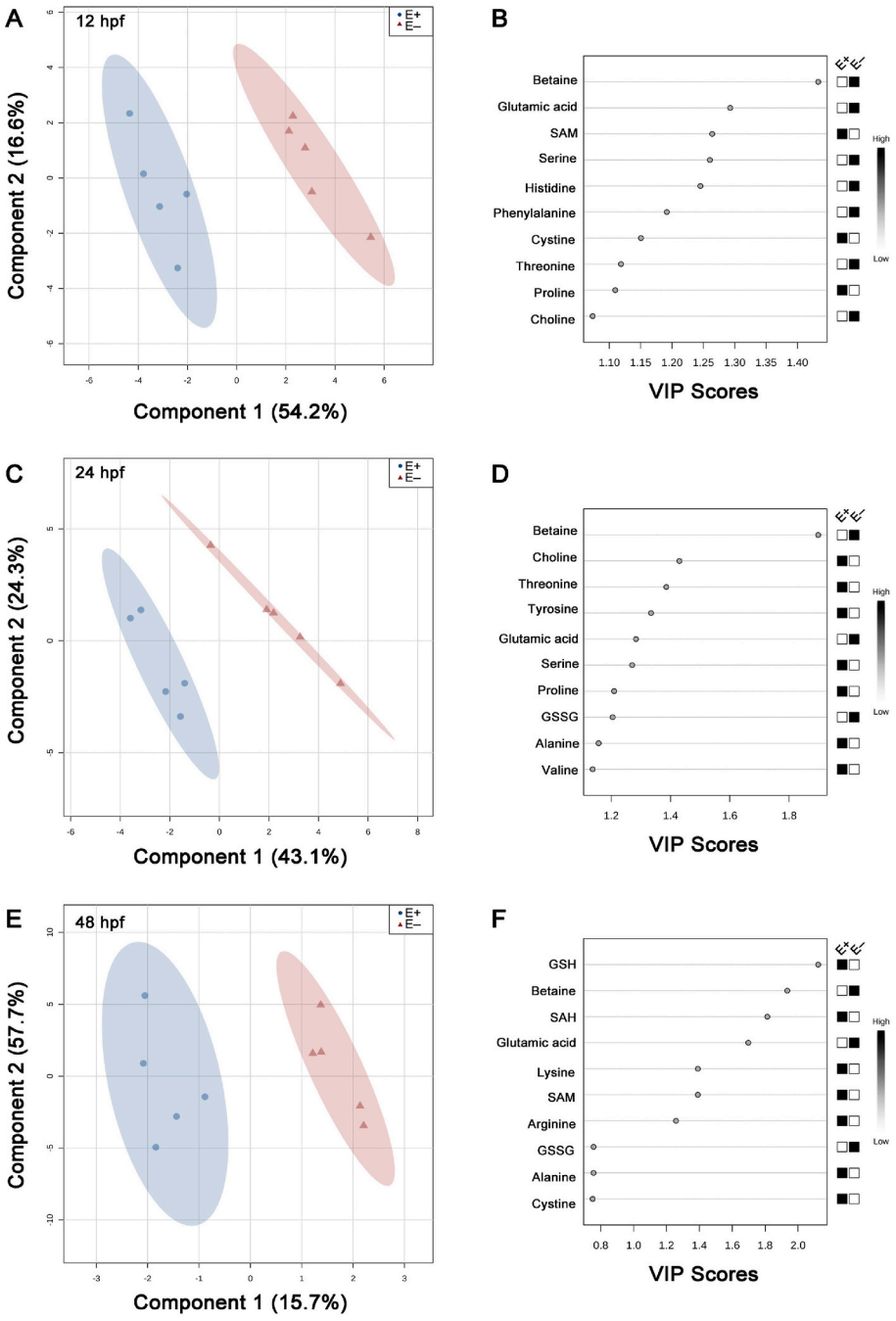

Fig. 2. Schematic representation of 2D PLS-DA scores plot and important features.
Metabolite features and concentrations from embryos (E+ and E−; n = 5 per group per time point per analysis) were normalized and assessed by partial least squares – discriminant analysis (PLSDA). 2D score plots were produced to separate feature differences between E+ and E− embryos at (A) 12-, (C) 24-, and (E) 48 hpf. E+ is shown in blue, E− is shown in red with corresponding 95% confidence regions (CR) drawn around each sample group. Variable importance of projection (VIP) scores from Component 1 of each PLS model indicate the most important features separating E+ and E− embryos at (B) 12-, (D) 24-, and (F) 48 hpf. Black and white boxes to the right of the VIP score plot indicate relative concentrations of each metabolite between E+ and E− embryos at the given time point.

Metabolite identification and quantification is further improved with the use of stable isotope-labeled AA, as an IS.

Zebrafish embryos are a closed system up to 5 days post-fertilization and do not obtain external nutrients. Prior to 48 hpf, the neural cord and brain are developed and segmented, and circulation initiates through closed circuits just before the first heart beat [18]. They, thus, are a valuable model of metabolic flux during early embryo development and lipid peroxidation arising during VitE deficiency before the presence of a fully formed liver. During this period, E− embryos experience greater incidence of developmental defects and delays indicated by reduced somites, bent axes and incomplete tail extension, and impaired brain and eye development. We therefore sought to determine the metabolic derangements associated with VitE deficiency during this critical developmental window. Previously, we observed choline depletion, methyl donor alterations and disturbed cellular energy metabolism in E− embryos [8,9]. These outcomes raise the question, “how is choline related to lipid peroxidation?” Choline is an integral part of phosphatidyl choline (PC), a membrane phospholipid, and we have shown that PC with docosahexaenoic acid (DHA-PC) is depleted in E− embryos [10]. To replace oxidized DHA-PC, PC can be synthesized from choline via the cytidine diphosphate-choline (CDP-choline) pathway or via the phosphatidylethanolamine-N-methyl transferase (PEMT) pathway [27]. The PEMT pathway uses methyl groups (SAM) to methylate phosphatidylethanolamine (PE) to form PC [27]. Overall, choline could be used directly in the CDP-choline pathway or could be converted to betaine for use in the methionine-Hcy cycle (Fig. 4). Our data shows that E− embryos contained increased betaine concentrations at all times investigated (12, 24 and 48 hpf; Fig. 4). Potentially, VitE deficiency up-regulates betaine production to increase available methyl groups, suggesting that those E− embryos that cannot maintain the

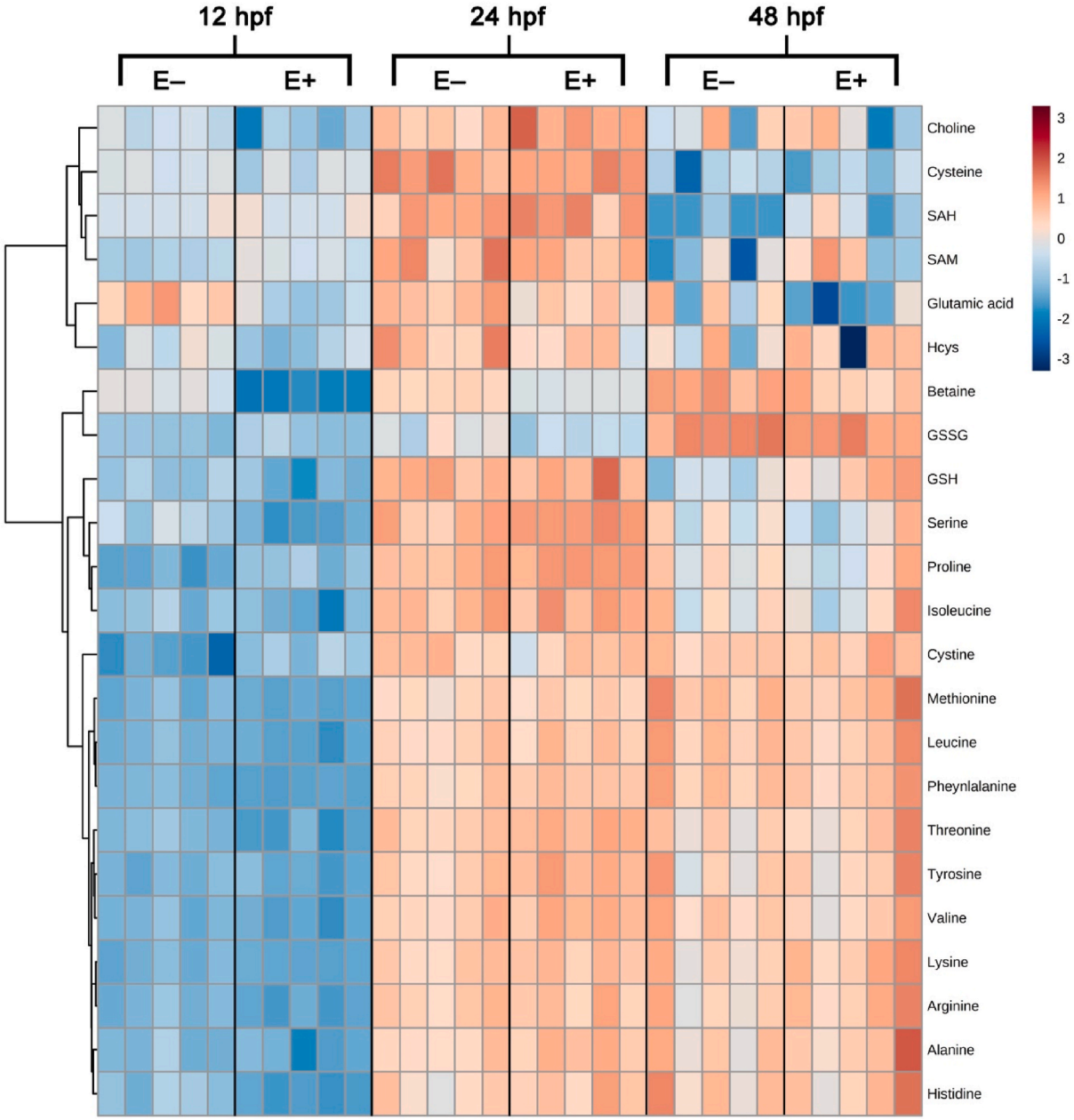

Fig. 3. Heatmap visualization of metabolite features and relative concentrations over time.
Metabolite features and concentrations from embryos (E+ and E−; n = 5 per group per time point per analysis) were normalized by log transformation and auto scaling. Heatmap was generated with Ward clustering algorithm and separated by Euclidean distance. Map is arranged by VitE status and time point with all measured metabolite features shown. Colored box to the right of the map indicates relative concentration of metabolite between E+ and E− embryos across all time points. Heatmap dendrogram separated primarily into two clusters by relative metabolite concentration: cluster one contains choline, cysteine, SAH, SAM, glutamic acid, and homocysteine with all other metabolites measured in cluster two. Cluster two is further separated by three family groups; one group contains betaine and GSSG, one group contains GSH, serine, proline and isoleucine, and one group contains the remaining 11 metabolites, which are primarily amino acids.

up-regulation of betaine production are unable to survive. Notably, betaine was a driver of differences between E+ and E− embryos as documented by the PLSDA analysis (Fig. 2B, D, F).

During VitE inadequacy, lipid peroxidation generates lipid hydroperoxides, which are reduced by phospholipid glutathione peroxidase (GPX4) using GSH [28]. To replace GSH, either energy (as NADPH) is required, or GSH could be synthesized de novo. γ-Glutamyl-cysteinyl synthase (γ-GSC) is the rate-limiting enzyme and cysteine the rate limiting amino acid for GSH synthesis. There are two cysteine sources [29]: 1) uptake of cystine in exchange for glutamate via the X_c^- exchanger, then cystine is reduced to cysteine, and 2) Hcy is redirected from the methionine cycle. In the present study, neither cystine nor cysteine concentrations were different between E+ and E− embryos at any time point, however, glutamate was significantly different ($P < 0.01$) at 12 and 48 hpf. These data suggest that the animal is generating a glutamate surplus to promote cysteine availability via the X_c^- exchanger. Nonetheless the attempt is futile because GSH by 48 hpf is significantly depleted (Fig. 4J, Table 1). Livers from rats fed a VitE deficient diet for 290 days were similarly depleted of total GSH with increases of γ-GCS transcription suggesting a lack of VitE increases genetic regulation of *de* novo GSH synthesis [30]. As shown by Timme-Laragy [19], total GSH increases during zebrafish embryo development, while the GSH/GSSG ratio fluctuates as a response to cellular differentiation and organogenesis. Thus, the inability of the E− embryos to maintain GSH at 48 hpf

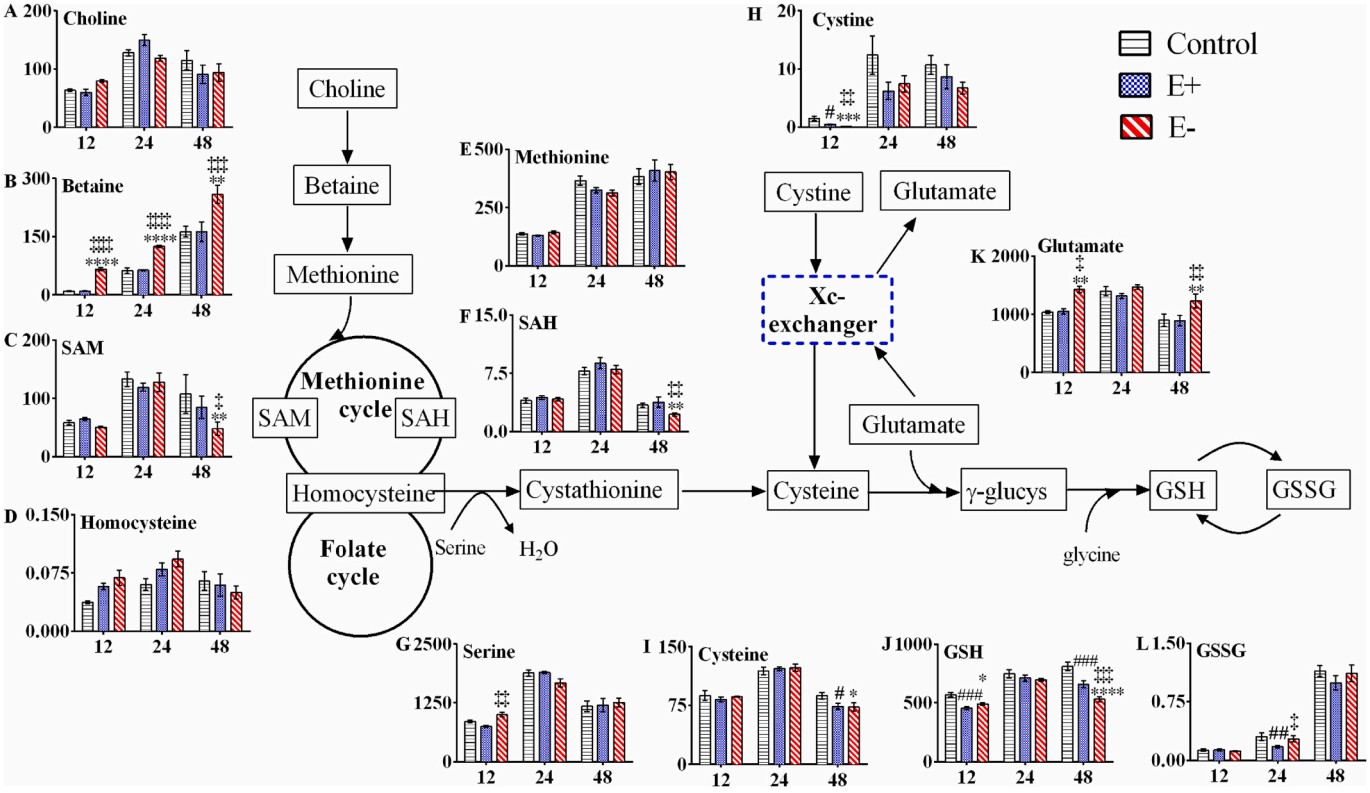

Fig. 4. Quantitative analysis of thiols, amino acids and related substances, Y-axes vary according to the concentration of each compound (pmol/embryo), X-axes shown times as 12, 24 and 48 hpf.

Embryos (E+, E− or control; n = 5 per group per time point per analysis) were analyzed either by the AA protocol (choline, betaine, SAM, SAH, methionine, serine and glutamate) and the thiol protocol (homocysteine, cysteine, cystine, GSH and GSSG). Data shown are pmol/embyro (mean ± SEM) at 12, 24 and 48 hpf. Symbols denote significant differences, as determined by Tukey post-hoc comparisons, at the time interval shown: E+ vs E− ‡$P \leq 0.05$, ‡‡$P \leq 0.01$, ‡‡‡$P \leq 0.001$, ‡‡‡‡$P \leq 0.0001$; control vs E− *$P \leq 0.05$, **$P \leq 0.01$, ****$P \leq 0.0001$; control vs E+ #$P \leq 0.05$, ##$P \leq 0.01$, ###$P \leq 0.001$. (A) Choline (Interaction, $P = 0.0670$, Time $P < 0.0001$, Group $P = 0.7725$), (B) Betaine (Interaction, $P < 0.0001$, Time $P < 0.0001$, Group $P < 0.0001$), (C) SAM (Interaction, $P = 0.2115$, Time $P < 0.0001$, Group $P = 0.0666$), (D) Homocysteine (Interaction, $P = 0.3539$, Time $P = 0.0802$, Group $P = 0.4504$), (E) Methionine (Interaction, $P = 0.3661$, Time $P < 0.0001$, Group $P = 0.7944$), (F) SAH (Interaction, $P = 0.0405$, Time $P < 0.0001$, Group $P = 0.0271$), (G) Serine (Interaction, $P = 0.0357$, Time $P < 0.0001$, Group $P = 0.4039$), (H) Cystine (Interaction, $P = 0.7759$, Time $P < 0.0001$, Group $P < 0.0001$), (I) Cysteine (Interaction, $P = 0.1655$, Time $P < 0.0001$, Group $P = 0.2320$), (J) GSH (Interaction, $P < 0.0001$, Time $P < 0.0001$, Group $P < 0.0001$), (K) Glutamate (Interaction, $P = 0.2791$, Time $P < 0.0001$, Group $P = 0.0001$), (L) GSSG (Interaction, $P = 0.0977$, Time $P < 0.0001$, Group P = 0.0622).

indicates that at this time they are undergoing severe redox stress and inadequate substrates. In the heat map (Fig. 3), GSH clustered with serine, proline and isoleucine, while Hcy, glutamate and cysteine clustered with methionine cycle related metabolites (choline, SAM and SAH). These findings suggest that Hcy may be diverted from the methionine cycle in the response to VitE deficiency. Nonetheless, the importance of cystine cannot be ruled out since it was a major variable in the VIP analyses (Fig. 2B, F).

The strength of this study is that we demonstrate using integrated analyses of the biochemical pathways in response to lipid peroxidation that the metabolic state of the E− embryos is disrupted early in development. The hierarchical clustering analyses provide valuable insights into these metabolic relationships. Although untargeted metabolomics assays show that these metabolites are dysregulated in the developing zebrafish embryo [8], the targeted analyses quantitate these changes. The limitations of the study are the complexity of the interrelations and the remaining challenge of unraveling the importance of each component. This study demonstrates that VitE deficiency alters overall thiol status in the developing embryo. Simultaneously, concentrations of the methyl donor, betaine, are greatly increased in the E− embryos. Betaine is thought to protect the pre-implantation human embryo by protecting epigenetic regulation via its methyl donation pathways [31]. However, betaine addition to culture medium of alcohol-treated mouse embryos suggested that betaine plays a role in protection from reactive oxygen species [32]. We suggest that betaine's critical role in the embryo is also to maintain thiol status. The quantitative analyses used here have provided some clues, but further flux analysis is necessary to define how specific metabolites change during embryogenesis. In summary, this study delivers a more accurate depiction of redox-sensitive thiols and the biochemical pathway disruption as a result of VitE deficiency in the developing zebrafish embryo.

Acknowledgements

The authors acknowledge the funding from the China Scholarship Council, who supported JZ. The Linus Pauling Institute and the Oregon State UniversityFoundation also supported this research. The research reported in this publication was partially supported by the National Institute of Environmental Health Sciences of the National Institutes of Health under Award P30ES030287. The content is solely the responsibility of the authors and does not necessarily represent the official views of the National Institutes of Health.

Appendix A. Supplementary data

Supplementary data to this article can be found online at https://doi.org/10.1016/j.redox.2020.101784.

References

[1] H.M. Evans, K.S. Bishop, On the existence of a hitherto unrecognized dietary factor essential for reproduction, Science 56 (1922) 650–651, https://doi.org/10.1126/science.56.1458.650.

[2] P.F. Surai, R.C. Noble, B.K. Speake, Tissue-specific differences in antioxidant distribution and susceptibility to lipid peroxidation during development of the chick embryo, Biochim. Biophys. Acta 1304 (1996) 1–10, https://doi.org/10.1016/s0005-2760(96)00099-9.

[3] G.T. Vatassery, C.K. Angerhofer, F.J. Peterson, Vitamin E concentrations in the brains and some selected peripheral tissues of selenium-deficient and vitamin E-deficient mice, J. Neurochem. 42 (1984) 554–558, https://doi.org/10.1111/j.1471-4159.1984.tb02713.x.

[4] G.W. Miller, L. Ulatowski, E.M. Labut, K.M. Lebold, D. Manor, J. Atkinson, C. L. Barton, R.L. Tanguay, M.G. Traber, The alpha-tocopherol transfer protein is essential for vertebrate embryogenesis, PloS One 7 (2012), e47402, https://doi.org/10.1371/journal.pone.0047402.

[5] G.R. Garcia, P.D. Noyes, R.L. Tanguay, Advancements in zebrafish applications for 21st century toxicology, Pharmacol. Ther. 161 (2016) 11–21, https://doi.org/10.1016/j.pharmthera.2016.03.009.

[6] K.M. Lebold, J.S. Kirkwood, A.W. Taylor, J. Choi, C.L. Barton, G.W. Miller, J. La Du, D.B. Jump, J.F. Stevens, R.L. Tanguay, M.G. Traber, Novel liquid chromatography-mass spectrometry method shows that vitamin E deficiency depletes arachidonic and docosahexaenoic acids in zebrafish (Danio rerio) embryos, Redox Biol 2 (2013) 105–113, https://doi.org/10.1016/j.redox.2013.12.007.

[7] G.W. Miller, E.M. Labut, K.M. Lebold, A. Floeter, R.L. Tanguay, M.G. Traber, Zebrafish (Danio rerio) fed vitamin E-deficient diets produce embryos with increased morphologic abnormalities and mortality, J. Nutr. Biochem. 23 (2012) 478–486, https://doi.org/10.1016/j.jnutbio.2011.02.002.

[8] M. McDougall, J. Choi, H.K. Kim, G. Bobe, J.F. Stevens, E. Cadenas, R. Tanguay, M. G. Traber, Lethal dysregulation of energy metabolism during embryonic vitamin E deficiency, Free Radic. Biol. Med. 104 (2017) 324–332, https://doi.org/10.1016/j.freeradbiomed.2017.01.020.

[9] M. McDougall, J. Choi, H.K. Kim, G. Bobe, J.F. Stevens, E. Cadenas, R. Tanguay, M. G. Traber, Lipid quantitation and metabolomics data from vitamin E-deficient and -sufficient zebrafish embryos from 0 to 120 hours-post-fertilization, Data Brief 11 (2017) 432–441, https://doi.org/10.1016/j.dib.2017.02.046.

[10] M.Q. McDougall, J. Choi, J.F. Stevens, L. Truong, R.L. Tanguay, M.G. Traber, Lipidomics and H2(18)O labeling techniques reveal increased remodeling of DHA-containing membrane phospholipids associated with abnormal locomotor responses in alpha-tocopherol deficient zebrafish (danio rerio) embryos, Redox Biol 8 (2016) 165–174, https://doi.org/10.1016/j.redox.2016.01.004.

[11] A.A. Moazzami, S. Frank, A. Gombert, N. Sus, B. Bayram, G. Rimbach, J. Frank, Non-targeted 1 H-NMR-metabolomics suggest the induction of master regulators of energy metabolism in the liver of vitamin E-deficient rats, Food & function 6 (2015) 1090–1097, https://doi.org/10.1039/c4fo00947a.

[12] S.L. Yang, S.S. Aw, C. Chang, S. Korzh, V. Korzh, J. Peng, Depletion of Bhmt elevates sonic hedgehog transcript level and increases beta-cell number in zebrafish, Endocrinology 152 (2011) 4706–4717, https://doi.org/10.1210/en.2011-1306.

[13] S. Prabhudesai, C. Koceja, A. Dey, S. Eisa-Beygi, N.R. Leigh, R. Bhattacharya, P. Mukherjee, R. Ramchandran, Cystathionine beta-synthase is necessary for axis development in vivo, Front Cell Dev Biol 6 (2018) 14, https://doi.org/10.3389/fcell.2018.00014.

[14] B. Head, J. La Du, R.L. Tanguay, C. Kioussi, M.G. Traber, Vitamin E is necessary for zebrafish nervous system development, Sci. Rep. 10 (2020) 15028, https://doi.org/10.1038/s41598-020-71760-x.

[15] C.B. Kimmel, W.W. Ballard, S.R. Kimmel, B. Ullmann, T.F. Schilling, Stages of embryonic development of the zebrafish, Dev. Dynam. 203 (1995) 253–310, https://doi.org/10.1002/aja.1002030302.

[16] K.M. Lebold, D.B. Jump, G.W. Miller, C.L. Wright, E.M. Labut, C.L. Barton, R. L. Tanguay, M.G. Traber, Vitamin E deficiency decreases long-chain PUFA in zebrafish (Danio rerio), J. Nutr. 141 (2011) 2113–2118, https://doi.org/10.3945/jn.111.144279.

[17] M. Podda, C. Weber, M.G. Traber, L. Packer, Simultaneous determination of tissue tocopherols, tocotrienols, ubiquinols, and ubiquinones, J. Lipid Res. 37 (1996) 893–901.

[18] M. Westerfield, The Zebrafish Book : a Guide for the Laboratory Use of Zebrafish (Brachydanio Rerio), University of Oregon Press, Eugene, OR, 2007.

[19] A.R. Timme-Laragy, J.V. Goldstone, B.R. Imhoff, J.J. Stegeman, M.E. Hahn, J. M. Hansen, Glutathione redox dynamics and expression of glutathione-related genes in the developing embryo, Free Radic. Biol. Med. 65 (2013) 89–101, https://doi.org/10.1016/j.freeradbiomed.2013.06.011.

[20] D. Jardine, M.K. Litvak, Direct yolk sac volume manipulation of zebrafish embryos and the relationship between offspring size and yolk sac volume, J. Fish. Biol. 63 (2003) 388–397, https://doi.org/10.1046/j.1095-8649.2003.00161.x.

[21] S. Uusi-Heikkilä, C. Wolter, T. Meinelt, R. Arlinghaus, Size-dependent reproductive success of wild zebrafish Danio rerio in the laboratory, J. Fish. Biol. 77 (2010) 552–569, https://doi.org/10.1111/j.1095-8649.2010.02698.x.

[22] T. Moore, A. Le, A.K. Niemi, T. Kwan, K. Cusmano-Ozog, G.M. Enns, T.M. Cowan, A new LC-MS/MS method for the clinical determination of reduced and oxidized glutathione from whole blood, J Chromatogr B Analyt Technol Biomed Life Sci 929 (2013) 51–55, https://doi.org/10.1016/j.jchromb.2013.04.004.

[23] H. Prinsen, B.G.M. Schiebergen-Bronkhorst, M.W. Roeleveld, J.J.M. Jans, M.G. M. de Sain-van der Velden, G. Visser, P.M. van Hasselt, N.M. Verhoeven-Duif, Rapid quantification of underivatized amino acids in plasma by hydrophilic interaction liquid chromatography (HILIC) coupled with tandem mass-spectrometry, J. Inherit. Metab. Dis. 39 (2016) 651–660, https://doi.org/10.1007/s10545-016-9935-z.

[24] ICH Expert Working Group ICH Harmonised Tripartite Guideline, Validation of analytical procedures: text and methodology Q2(R1). International Conference on Harmonisation of Technical Requirements for Registration of Pharmaceuticals for Human Use, 2005, p. 17.

[25] Pang, Z.; Chong, J.; Li, S.; Xia, J. MetaboAnalystR 3.0: toward an optimized workflow for global metabolomics. Metabolites 10; 2020, doi: 10.3390/metabo10050186.

[26] I.T. Jolliffe, J. Cadima, Principal component analysis: a review and recent developments, Philos Trans A Math Phys Eng Sci 374 (2016) 20150202, https://doi.org/10.1098/rsta.2015.0202.

[27] C.J. DeLong, Y.J. Shen, M.J. Thomas, Z. Cui, Molecular distinction of phosphatidylcholine synthesis between the CDP-choline pathway and phosphatidylethanolamine methylation pathway, J. Biol. Chem. 274 (1999) 29683–29688, https://doi.org/10.1074/jbc.274.42.29683.

[28] F. Ursini, M. Maiorino, Lipid peroxidation and ferroptosis: the role of GSH and GPx4, Free Radic. Biol. Med. 152 (2020) 175–185, https://doi.org/10.1016/j.freeradbiomed.2020.02.027.

[29] G.J. McBean, The transsulfuration pathway: a source of cysteine for glutathione in astrocytes, Amino Acids 42 (2012) 199–205, https://doi.org/10.1007/s00726-011-0864-8.

[30] L. Barella, P.Y. Muller, M. Schlachter, W. Hunziker, E. Stocklin, V. Spitzer, N. Meier, S. de Pascual-Teresa, A.M. Minihane, G. Rimbach, Identification of hepatic molecular mechanisms of action of alpha-tocopherol using global gene expression profile analysis in rats, Biochim. Biophys. Acta 1689 (2004) 66–74, https://doi.org/10.1016/j.bbadis.2004.02.002.

[31] S.A. Craig, Betaine in human nutrition, Am. J. Clin. Nutr. 80 (2004) 539–549, https://doi.org/10.1093/ajcn/80.3.539.

[32] D. Zhang, H. Jing, C. Dou, L. Zhang, X. Wu, Q. Wu, H. Song, D. Li, F. Wu, Y. Liu, W. Li, R. Wang, Supplement of betaine into embryo culture medium can rescue injury effect of ethanol on mouse embryo development, Sci. Rep. 8 (2018) 1761, https://doi.org/10.1038/s41598-018-20175-w.